Assessment of Influencing Factors in Decentralized Energy Supply of Manufacturing Industries Using Probabilistic Methods

Heiko Dunkelberg*, Henning Meschede, Fabian Stöhr, Jens Hesselbach

Department for Sustainable Products and Processes, Institute of Production Technology and Logistics, University of Kassel, Hesse, Germany; *dunkelberg@upp-kassel.de

SNE 27(2), 2017, 67 - 76, DOI: 10.11128/sne.27.tn.10372
Received: May 25, 2017
Accepted: June 10, 2017 (Special Issue Review)
SNE - Simulation Notes Europe, ARGESIM Publisher Vienna
ISSN Print 2305-9974, Online 2306-0271, www.sne-journal.org

Abstract. Plastics industry is the ninth largest electrical energy consuming sector in Germany. Currently, the production including the melting of plastic is electricity based although decentralized energy supply concepts using CHP units and thermal energy for melting and cooling exist. This research analyses the influencing factors 'production plan' and 'ambient temperature'. For both parameters, the influence on the decentralized energy concept and the status quo is compared. Therefore real data is used to parameterize probabilistic density functions. The system's behaviour by means of varying input profiles is evaluated using Monte-Carlo simulation. The results show that the influence of the production plan is stronger than the influence of the ambient temperature. Moreover the influence increases for the decentralized energy supply scenario.

Introduction

Considering the energy demand, plastics industry is the ninth largest electricity consuming sector in Germany [1]. The production process of injection moulded parts is very energy intensive.

Plastics industry is characterized by energy costs amounting to 1,8 % of their turnover [2]. The specific energy consumption is 0,78 MWh_{el}/t [3].

The German Association of the Plastics Converters (GKV) lists 2.800 plastic processing companies which exclusivly process plastics [4]. About one third of them are injection moulding companies. Including in-house moulders the number of companies which have their own injection moulding line is 2.300 [5].

In general, plastics processing companies use almost 100 % electricity to cope with their energy demand, excluding those companies which operate combined heat and power (CHP) systems.

Almost 50 % of the electricity is used either for the drive of the injection moulding machines or to apply clamping forces. Additional 15 % of electricity is needed for heating the plasticizing cylinder for melting the plastic as well as the hot runner system. The total energy demand for cooling is about 15 % while the system is usually separated in two cooling circuits. The first circle is used for cooling the molten plastic to 14 °C. In this case, compression chillers in combination with a dry cooler with winter relief are used. The other circle cools the machine drives and components. The temperature level is about 30 °C [6]. In Germany, dry coolers or cooling towers can be used all over the year. The remaining percentage of electricity is used for handling systems, lightning, the supply of compressed air and the drying of plastics. Depending on the material and produced product, the distribution of energy may change [7].

Current research activities focus on decentralized energy supply concepts for industries to reduce environmental impacts like greenhouse gas emissions. Schlüter describes the implementation of a trigeneration system in addition with thermal oil instead of electricity for heating the cylinders and melting plastics [6]. Dunkelberg et al. showed a thermal oil concept for extruders and its technical application as well as established the technical feasibility [8]. Wagner et al. evaluated energetically different scenarios of decentralized energy concepts in the plastic industry with focus on the link between production process and production hall [9].

The state-of-the-art design of new energy systems is based on standard load and temperature profiles.

Heat and cold generators as well as CHP plants are mostly designed in the same way by using load duration curves. Probabilistic variations of load or temperature around the years are seldom considered while extreme value scenarios like full production and highest temperature are performed. This leads to oversizing or non-optimal dimensioning.

In this research, a decentralized energy supply system for the plastic industry is investigated. To evaluate the feasibility of the concept, the production schedules as well as the ambient temperature are simulated as Probability Density Functions (PDF) to generate various probabilistic scenarios. This approach allows the determination of the resilience of decentralized energy concepts and an evaluation of the concept's sensitivity towards these two influencing parameters.

1 Methodology

1.1 Monte-Carlo Algorithm

In general Monte-Carlo methods are algorithms which use random inputs. They can be used to simulate complex stochastic models and generate data series with typical conditions and trends [10]. They are applied to different areas such as physics, economics, medicine and engineering.

The stochastic influences of technical and economic systems are often modelled by Probability Density Functions or Markov Chains. Pereira et al. analysed the Net Present Value (NPV) and produced energy cost of a photovoltaic (PV) system in Brazil based on PDF of total initial costs, interest rate and price per kWh sold to utility [11]. Nijhuis et al. used a Markov Chain approach to simulate residential occupancy figures as well as PDF of user behaviour and weather data to develop electricity load profiles [12]. Arun et al. investigated the optimal battery size for PV systems based on probabilistic electricity load profiles and a normally distributed PDF of solar radiation [13]. Further, Roy et al. developed a sizing curve for standalone wind-battery systems. Taken into account are the electricity load profile and the uncertainity of wind by Weibull PDF [14]. Sharafi and El Mekkawy used different PDF of weather data and load profiles to simulate a hybrid renewable energy supply of an apartment in Canada. Finally, they made a sensitivity analysis of various influence parameters [15].

1.2 Ambient temperature

A common procedure to generate synthetic weather data is to use Markov chain [16-19]. They are suitable to describe stochastic processes if a lot of historic data is available. An introduction into Markov chains and their application can be found in [20].

In this paper we introduce an approach using first order Markov chains to generate hourly ambient temperature time series. Based on historic weather data various transition probability matrices (TPM) are defined. They are divided by three categories: month, hourly amount of solar radiation and trend of solar radiation compared to the previous hour. The amount of solar radiation is combined in radiation classes of 100 W/m² each. A radiation of 0 W/m² forms its own class. The trend can be positive, negative or neutral. For a maximum solar radiation of 1.000 W/m² this results into 396 different TPM.

The column index of each TPM represents the temperature of the previous time step. Each element p_{nm} in a column stands for the cumulative probability of the current ambient temperature (ϑ_{amb}), represented by the rows. The principle setting of the TPM of temperature is shown in Figure 1.

$$\begin{array}{c} \\ \vartheta_{amb,1}^{t} \\ \vartheta_{amb,2}^{t} \\ \vartheta_{amb,3}^{t} \\ \vdots \\ \vartheta_{amb,n}^{t} \end{array} \begin{array}{c} \begin{array}{cccccc} \vartheta_{amb,1}^{t-1} & \vartheta_{amb,2}^{t-1} & \vartheta_{amb,3}^{t-1} & \cdots & \vartheta_{amb,m}^{t-1} \end{array} \\ \begin{bmatrix} p_{11} & p_{12} & p_{13} & & p_{1m} \\ p_{21} & p_{22} & p_{23} & \ldots & p_{1m} \\ p_{31} & p_{32} & p_{33} & & p_{1m} \\ \vdots & \vdots & & \ddots & \\ p_{n1} & p_{n2} & p_{n3} & \ldots & p_{nm} \end{bmatrix} \end{array}$$

Figure 1: Principle setting of TPM.

To generate the time series, the ambient temperature of the first hour is randomly chosen in the range of possible temperatures. Then, depending on the month, solar radiation class and trend, the corresponding TPM is selected.

With the temperature of the previous time step and randomly chosen probability, the TPM is used to generate the current ambient temperature. Finally, the time series gets corrected to reduce the variability. Therefore a simple moving average (SMA) is formed.

The pseudocode for the function $\vartheta_{\mathrm{amb}} = \mathrm{f}(\mathrm{G_h})$ is presented below:

```
for t = 1:simulation time
% determine month of the year (moy)
    moy = month(t)
% determine the solar rad. class (SRC)
% by using global radiation (G_h^t)
    SRC = G_h^t / 100
% determine solar radiation trend (SRT)
    if G_h^t - G_h^(t-1) > 0
        SRT = 1
    Else if G_h^t - G_h^(t-1) < 0
        SRT = -1
    else
        SRT = 0
    end
% find corresponding TPM
    TPM = TPM(moy, SRC, SRT)
% chose corr. column tpp of TPM
    tpp = TPM(ϑ_amb^(t-1))
% chose a random variable R = [0,1]
% determine ϑ_amb^t
    ϑ_amb^t = row(tpm = p_n) with p_n ≤ R & p_(n-1) > R
end

% perform SMA for reducing variability
for i=1: simulation time
    ϑ_amb^t = 1/5 Σ_(i=-2)^2 ϑ_amb^(t+i)
end
```

Listing 1: Generation of probabilistic temperature profile.

To generate a synthetic time series of solar radiation an approach according to Duffie and Beckman [21] can be used.

1.3 Energy needs

For further simulations probabilistic parameter sets of the energy demand of injection moulding machines have been created. The energy demand of the machines depends on the temporal machine's state. There are four different machine states, which depend on different inputs and parameters like type of machine and melt or production programme:

- *Automatic mode*: The machine produces autonomously parts without interventions of the machine operators.
- *Manual mode:* The machine operator controls the machine. Cycle time and machine performance are specified by the operator. Compared to the automatic mode the performance is lower.
- *Alarm mode:* The machine has identified an error and is changed to the standby position. Important components are held at a certain temperature.
- *Offline mode:* The machine is switched off and does not produce.

The transition between the operating conditions of single machines has been analysed and shown by transition probabilities. The probabilistic parameter sets of the energy demands for power, heating and cold base on real data sheets of a medium sized plastics factory. Individual sets of sequences of states are generated for each machine. A part of the TPM of machines is shown in Figure 2.

	Long – runner				...	*runner n*
	State 1	*State* 2	*State* 3	*State* 4	⋯	*State n*
State 1	0,18	0,80	0,04	0,00	⋯	TP_{1n}
State 2	0,65	0,90	1,00	0,97	⋯	TP_{2n}
State 3	1,00	0,96	1,00	0,97	⋯	TP_{3n}
State 4	1,00	1,00	1,00	1,00	⋯	TP_{4n}

Figure 2: Part of the TPM of machine states.

Similar machines have been classified into four different groups:

- *Long-runner*: The production time is longer than 80 % of the possible production time. The production is interrupted only by short alarm and offline times.
- *Short-runner*: The production time of the machine is shorter than 40 % of the possible production time.
- *Normal-runner-offline*: The production time is by nearly 60 %. Production is interrupted by few but long offline times.
- *Normal-runner-cycle*: The production time is by nearly 60 %. Production is interrupted by many short offline times.

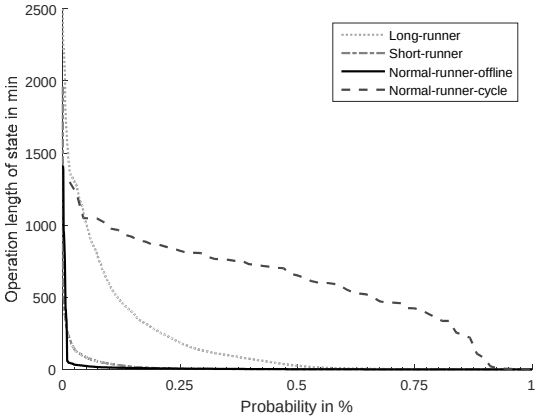

Figure 3: Runtime of the machine groups.

An exemplary description of probabilistic operation lengths for different types of machines is shown in Figure 3.

Furthermore, machines are classified into four different performance classes. The performance data results from measurements and describes the specific energy consumption and cooling needs of each machine. The process data are provided by a host-computer system.

For the parameter sets, probabilistic machine operation states are generated in accordance to the following procedure shown in Figure 4.

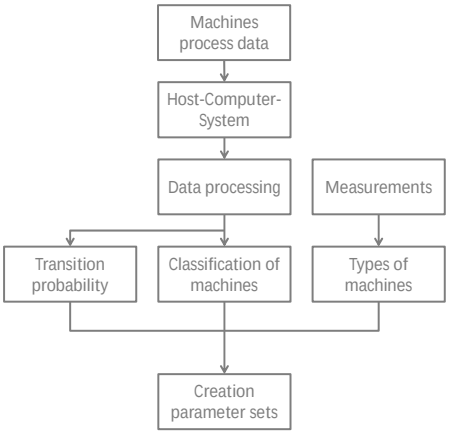

Figure 4: Procedure for creating parameter sets.

The operation states have been combined with the performances for the operation state and the machine type. As a result there are probabilistic load profiles. The pseudocode is presented below:

```
% determine number of active machines M
% of all installed machines M_set
     M = M_set ± 20 %
% initialize first state s_m^i with i = 0
    for m = 1:M
% while cumulated machine run time t_m
% shorter than simulation time t_s
        while t_m < t_s
% chose PDF of machine group and state
% chose a random variable
        R_1 = [0,1]
% determine duration of state d_m^i with
% corresponding PDF and random number
        d_m^i = PDF(R_1)
% find corr. TPM of actual state tpp
        tpp = TPM(s_m^i)
% chose a random variable
        R_2 = [0,1]
% determine new state of the machine s_m^(i+1)
        s_m^(i+1) = tpp(R_2)
% calculate energy demand vector E_m^i
% depending on state
          E_m^i = f(s_m^i, d_m^i)
          i = i+1
    end
end
```

Listing 2: Generation of probabilistic load profile.

2 Simulation Model

2.1 Description of the modules

Besides climatic and energetic input data, the simulation model consists of different modules for cooling and heating which are modelled as follows.

Dry cooler. The dry cooler (DC) uses the ambient temperature to cool down the circuit via fans. It is assumed that the installed capacity is sufficient for removing all the heat. Thus, the cooling output of the dry cooler only depends on the ambient temperature. If the ambient temperature is lower than the upper limit temperature of the dry cooler, the cooling output is equal to the cooling demand; otherwise the cooling output $\dot{Q}_{cool}$ is equal zero (equation 1):

$$6\dot{Q}_{cool,DC} = \begin{cases} \dot{Q}_{cool}, & \vartheta_{amb} < \vartheta_{max,DC} \\ 0, & \vartheta_{amb} \geq \vartheta_{max,DC} \end{cases} \quad (1)$$

The electric consumption of the dry cooler depends on the cooling output and the energy efficiency ratio (EER), which is set constant (equation 2):

$$P_{DC} = \dot{Q}_{cool,DC} \Big/ EER_{DC} \quad (2)$$

Compression chiller. The compression chiller cools down the circuit via vapour compression using electricity. Cooling output and power input are connected by the EER (equation 3):

$$P_{CCM} = \dot{Q}_{cool,CCM} \Big/ EER_{CCM} \quad (3)$$

According to Schlüter the EER can be calculated as a product of a basis EER, a factor depending on the ambient temperature and a factor depending on the cooling temperature [6]. In addition to this, a further factor is introduced to represent the dependence on the partial load performance (equation 4):

$$EER_{CCM} = EER_{basis} * \prod f_i \quad (4)$$

Trigeneration plant. The combined cooling, heating and power system (CCHP) uses a natural gas engine to generate electricity. The natural gas (NG) input depends on the partial load of the engine; the function is shown in Table 1.

	Part load			
	0 %	50 %	75 %	100 %
Fuel consumption	0 %	59 %	80 %	100 %

Table 1: Fuel consumption in part load in percent of full load value.

Furthermore the CCHP unit provides heat; either by the exhaust gas or by the cooling cycle of the engine. Moreover, the plant produces cooling via absorption chilling. Hereby, a part of the heat is converted into cooling. The functional description of the EER of the absorption chiller is taken from Schlüter [6]. Following the determination of the EER of the compression chiller, the EER of the absorption chiller depends on the ambient temperature, on the cooling temperature and moreover on the re-cooling temperature. The re-cooling temperature is calculated by the following equation with a constant efficiency η (equation 5):

$$\vartheta_{f,out} = \vartheta_{f,in} - \eta(\vartheta_{f,in} - \vartheta_{amb}) \quad (5)$$

where $\vartheta_{f,out}$ is the fluid outlet temperature and $\vartheta_{f,in}$ the fluid inlet temperature in °C.

Burner. The burner uses natural gas to provide heat. The natural gas amount is calculated by a constant efficiency (equation 6):

$$\dot{m}_{NG,burner} = \dot{Q}_{heat,burner} / \eta_{burner} \quad (6)$$

where $\dot{m}_{NG,burner}$ is the mass flow of natural gas in kg/hr, $\dot{Q}_{heat,burner}$ the thermal output in W and η_{burner} the burner's efficiency.

2.2 Analysed scenarios

Two different stages of decentralized energy supply scenarios are modelled using Matlab / Simulink. For simulation reasons, the signal routing shown in the following figures is opposing the energy flow. The first system describes the state of the art of energy supply for plastic industries and is shown in Figure 5.

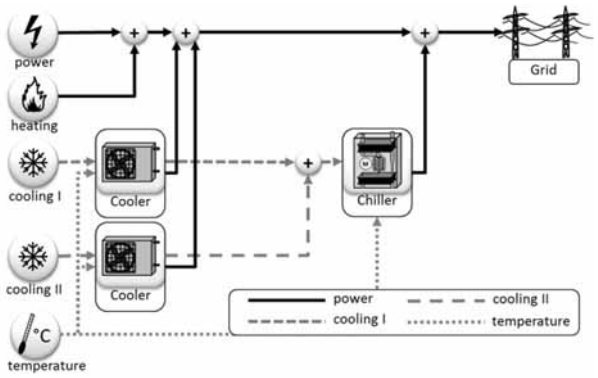

Figure 5: Signal routing Matlab Simulink model state of the art of energy supply in plastic industries.

The system consists of the injection moulding machines, demanding different forms of energy: heat for the melting, electricity for the drive, cooling for the tool and cooling for the drive. The heat for the melting is generated electrically. Due to this the heat demand is converted into an electricity demand.

The drive cooling is achieved using a dry cooler. In case of ambient temperatures higher than 11 °C the system is not able to cool down the circuit and a compression chiller provides the cooling. The cooling for the drive is realized by a further dry cooler. Above an ambient temperature of 30 °C the cooling has to be realized by the compression chiller, too.

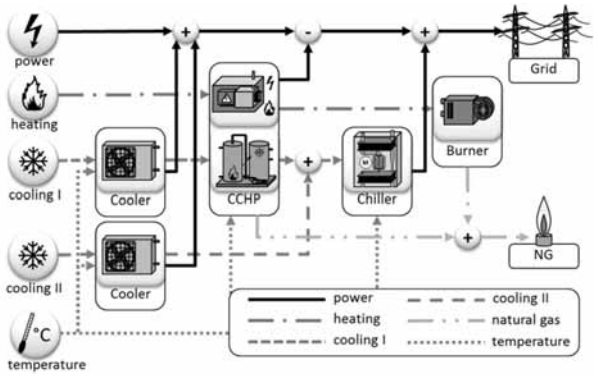

Figure 6: Signal routing Matlab Simulink model full decentralized energy supply in the plastic industries.

Instead of the electric heating of the melting process a thermal oil system is integrated in this second system (Figure 6). The thermal oil system is explained in detail in Schlüter [6]. Furthermore, a CCHP system is added which performs according to the cooling demand of the injection moulding machines.

The generated electricity is used for the drives whereas the heat of the exhaust gas is partly used for heating thermal oil to satisfy the heat demand. Together with the heat of the engine cooling circuit the other part of the exhaust gas heat drives an absorption chiller to satisfy the cooling demand of the melt in cases of ambient temperatures higher than 11°C. The compression chiller is still included as a back-up system. Furthermore, a natural gas burner is integrated in the thermal oil system in cases of less heat generation by the CCHP system. Finally the system is bidirectionally linked to the grid.

2.3 System configuration

The design of the energy supply is based on a companies' thermal and electrical load profiles. A data set for 40 injection moulding machines is generated according to the approach shown in Figure 4. Two exemplary sets of parameters are considerd and simulated. Set 1 includes only machines of type "Long-runner". It represents a factory with high machine running times which is typical for a custom moulder which produces technical components for the automotive industry. Machines of different types are simulated in set 2. It represents the industry average and corresponds to the investigated company. The distribution is shown in Table 2 and 3.

In accordance with the state-of-the-art, the CCHP system is designed using standard weather data and a standard load profile for the energy consumption. The performance of the CCHP is led by the cooling demand which has to be covered by the absorption chiller, i.e. the total cooling demand reduced by the cooling performance of the dry coolers.

	Long runner	Short runner	Normal offline	Normal cycle
Type 1	10	0	0	0
Type 2	5	0	0	0
Type 3	10	0	0	0
Type 4	15	0	0	0

Table 2: Number of machines for the system configuration dataset 1.

The state-of-the-art design uses standard weather data to determine the resulting cooling load. With regards to economic feasibility, the minimal full load hours of the absorption chiller are set to 4000 hr/y. The CHP unit is designed to the resulting heat load.

This leads to a CHP fuel input of 400 kW. The resulting absorption chilling machine (ACM) performance is approx. 120 kW_{th}. The thermal output for the thermal oil is set to 15 % of the fuel use. The gas burner is designed to ensure the remaining heat power for the thermal oil. The dry cooler and the compression chilling machine (CCM) are able to satisfy the total cooling load.

	Long runner	Short runner	Normal offline	Normal cycle
Type 1	10	0	0	0
Type 2	0	5	0	0
Type 3	0	0	5	5
Type 4	10	0	0	5

Table 3: Number of machines for the system configuration dataset 2.

2.4 Implementation of the simulation

To determine the influence of probabilistic distributed load and temperature profiles to the simulation results, the scenario analysis is divided into sub-scenarios. For this purpose the load as well as the temperature profiles have been fixed.

For this reason the parameters' influences are analysed and compared to each other. All possible combinations have been simulated. The analysed combinations are shown below:

a. fixed load profile and fixed temperature profile
b. variable load profile and fixed temperature profile
c. fixed load profile and variable temperature profile
d. variable load profile and variable temperature profile

Because of the dependence of the ambient temperature, three representative months are chosen to evaluate the results in winter and summer as well as in a transition period.

3 Results

Comparing the mentioned sub-scenarios b. and c., the results show that the influence of a variable load profile is more sensitive than a variable temperature profile. For this reason, only the sub-scenarios c. and d. are presented in the following.

3.1 Status quo scenarios

The results of the simulation runs of the status quo system using dataset 1 (only long runners) are presented in the following figures. Each figure consists of four histograms, each presenting one of the following indicators:

1. *Machines:* Electricity consumption of machines
2. *Grid:* Electricity consumption from public grid
3. *CCM:* Electricity consumption of *CCM*
4. *Primary energy:* Primary energy consumption of whole system

For the same sub-scenario, the histogram of the electricity consumption of the machines is not changing. Figure shows exemplary the distributions of the indicators for the summer season with fixed load and variable temperature while Figure 8 shows those for summer season with variable load and variable temperature.

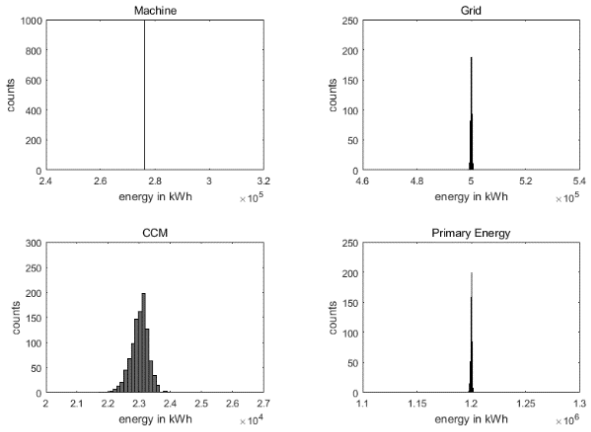

Figure 7: Distribution of indicators for summer season with fixed load and variable temperature.

It is apparent that the distribution range of each indicator becomes wider in the scenarios with variable load profile. Regarding the primary energy consumption, the range increases from 4.700 kWh to 156.200 kWh while the mean value is nearly the same (1.200.000 kWh respectively 1.208.000 kWh). This behaviour underlines the strong influence of the probabilistic distributed load profile to the simulation results.

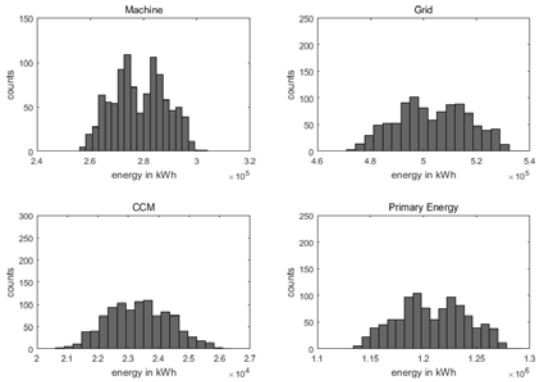

Figure 8: Distribution of indicators for summer season with variable load and variable temperature.

3.2 Decentralized energy supply scenarios

The following shows the results from the simulation runs of the decentralized energy supply with the dataset 1 (only long-runners). To evaluate the system's behaviour and the parameters' influence, six energetic indicators are used for benchmarking:

1. *Machines:* Electricity consumption of machines
2. *CCHP:* Electricity generation of CHP unit
3. *Grid:* Electricity consumption from public grid
4. *ACM:* Electricity consumption of ACM
5. *CCM:* Electricity consumption of CCM
6. *Primary energy:* Primary energy consumption of whole system

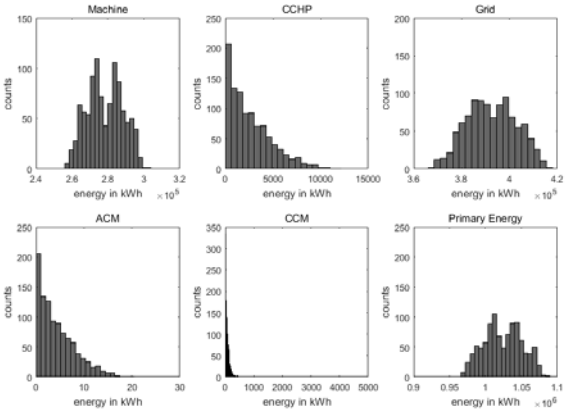

Figure 9: Distribution of indicators for winter season with variable load and variable temperature.

The results of chosen sub-scenarios are shown in figures consisting of six histograms, each representing one indicator. For the same sub-scenario, the histogram of the electricity consumption of the machines is not changing. Figure 9 shows exemplary the distributions of the indicators for the winter season with variable load and variable temperature while Figure 10 shows those for summer season with variable load and variable temperature.

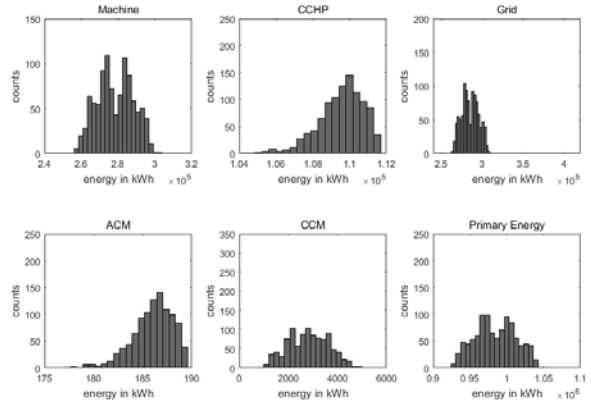

Figure 10: Distribution of indicators for summer season with variable load and variable temperature.

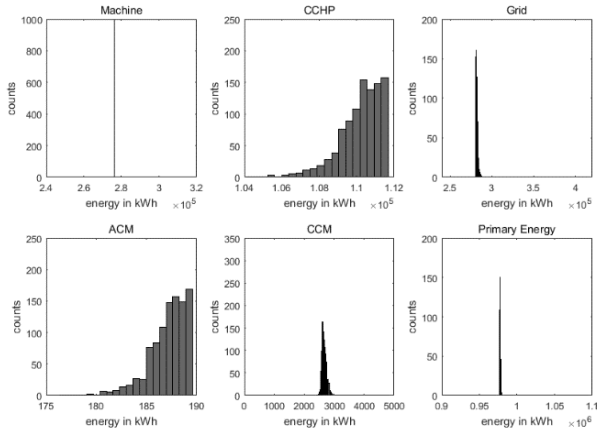

Figure 11: Distribution of indicators for summer season with fixed load and variable temperature.

In all simulated scenarios it is obvious that during the winter season the electricity consumption from public grid is at the highest level compared to the other periods, although the electricity consumption for the compression chiller is at its lowest level close to zero.

The comparison of the primary energy consumption of both seasons underlines that from a holistic and systemic point of view, in such a system the utilisation of the CHP unit instead of the operation of dry coolers is preferred because of the reduced electricity consumption from the grid. Furthermore, the comparison between both scenarios shows that in any case the decentralized system has significant primary energy savings. The primary energy factor for electricity is 2.4 and for gas 1.1 [22]. Especially the factor for electricity might change with higher share of renewable energies in the grid.

Comparing the distribution of indicators for summer season with variable load and variable temperature with those of summer season with fixed load (shown in Figure 11) allows the evaluation of the sensitivity of the influencing parameters.

The mean value of the CHP unit's electricity generation shifts slightly to the right. The same happens with the mean value of the absorption chiller's electricity consumption. This behaviour underlines that the full load hours of both systems increase by using a fixed load profile. Regarding the design process of the CHP unit shows that the utilization of standard load profiles can lead to an oversizing of the system. That means that the ACM and the CHP as well may not work at the optimum operating point.

Considering the three indicators electricity consumption from the grid, electricity consumption of the compression chiller and primary energy consumption of the whole system, the comparison of Figure 10 and Figure 11 illustrates that the range of these indicators become smaller while the mean values are nearly the same. In detail, for the single indicators the width of the range changes from 130.700 kWh to 2.810 kWh (primary energy), 4.059 kWh to 490 kWh (compression chiller) and 47.930 kWh to 7.480 kWh (consumption from public grid). This behaviour shows that the influence of probabilistic load profile is higher than the influence of probabilistic temperature data.

Comparing the simulation results of dataset 2 with dataset 1 it is obvious that there is an influence by the machines types to the results. The distribution is similarly to the distribution of dataset 1. It can be seen that the mean of the distribution is shifted and the width of range is smaller. For example for summer seasons the mean changes from 984.700 kWh to 961.000 kWh (primary energy). The width of range changes from 130.000 kWh to 94.300 kWh (primary energy).

4 Conclusion

The influence of probabilistic data on decentralized energy supply systems for the plastic industry depends on the parameter and the season. The highest influence is in the summer season. Furthermore, a probabilistic distributed load profile affects the result stronger than varying temperature profiles. In comparison to the results of the status quo system the influence of the parameters in the simulation of the decentralized system is stronger. For example, the change of width of the primary energy consumption from sub-scenario fixed load and variable temperature to both variable profiles is 33,23 % for the status quo but 46,51 % for the decentralized system.

The investigation shows also that the state-of-the-art design process of such energy systems allows good and fast results. Nevertheless, the Monte-Carlo simulation underlines that the designed configuration is oversized in some cases. Furthermore, in respect to extreme value scenarios, the Monte-Carlo simulation indicates the probability of such events and that these scenarios occur very rarely for short a time period.

On going research focuses on the transferability to other sectors with different influencing factors is examined. It is also considered how the presented approach can be applied for large scale energy systems with more than one consumer.

Furthermore, the data provided by measurements and the computer host system could be replaced by a previous simulation models. To get the PDF of the energy needs this model has to consider probabilistic inputs, too.

5 Acknowledgments

The authors would like to thank the Federal Ministry for Economic Affairs and Energy (BMWi) for the financial support of the project Smart Consumer (FKZ: 03ET1180).

References

[1] Rohde C. *Erstellung von Anwendungsbilanzen für das Jahr 2012 für das verarbeitende Gewerbe mit Aktualisierungen für die Jahre 2009-2011:* Studie für die Arbeitsgemeinschaft Energiebilanzene.V. (AGEB) - Entwurf. Karlsruhe; 2013. 40 p.

[2] EnergieAgentur.NRW. *Energieeffizienz-Kunststoffverarbeitende Industrie*. 2015; Available from: http://www.energieagentur.nrw/energieeffizienz/energieeffizienz-nach-branchen/energieeffizienz-kunststoffverarbeitende-industrie. (online: June 24, 2016).

[3] Bayerisches Landesamt für Umweltschutz. *CO2-Minderung durch rationelle Energienutzung in der Kunststoffverarbeitenden Industrie.* Augsburg: Bayerisches Landesamt für Umweltschutz; 2002. 85 p.

[4] GKV Gesamtverband Kunststoffverarbeitende Industrie e.V. *Kunststoffverarbeitung 2015 Betriebe mit 20 und mehr Beschäftigten*. 2015; Available from: http://www.gkv.de/de/statistik.html. (online: June 24, 2016)

[5] Applied Market Information Ltd. AMI Publications / Market Data, *AMI's Database of Injection Moulders in Germany 2013*. 8. Bristol, England: Applied Market Information Ltd, 2013. 287 p.

[6] Schlüter A. *Beitrag zur thermischen Energieversorgung in der Kunststoffverarbeitung - Systemische Lösungen und Potenziale* [dissertation]. [umweltgerechte Produkte und Prozesse, (Ger)]. University of Kassel; 2013.

[7] Gonser J. *Umweltschutz in der Kunststoffverarbeitung.* Berlin: Senatsverwaltung für Stadtwentwicklung; 2000. 43 p.

[8] Dunkelberg H, Rommel B, Hesselbach J. Der thermoöltemperierte Extruder. *Kunststoffe*. 2016; 10: 223-228.

[9] Wagner J, Dunkelberg H, Hannen C, Schlüter A, Phan L, Hesselbach J et al. Decreasing the Primary Energy Demand in the Plastics Industry by Modifying and Linking Energy Flows. *Proceedings of the 2016 ASHRAE Annual Conference 2016;* 2016 June; St. Louis USA. Proceedings of the 2016 ASHRAE Annual Conference: ASHRAE.

[10] Müller-Gronbach T, Novak E, Ritter K. Monte Carlo-Algorithmen. Berlin Heidelberg: Springer-Verlag; 2012. 324 p.

[11] Pereira, Edinaldo José da Silva, Pinho JT, Galhardo MAB, Macêdo WN. Methodology of risk analysis by Monte Carlo Method applied to power generation with renewable energy. *Renewable Energy* 2014; 69: 347-355.

[12] Nijhuis M, Gibescu M, Cobben J. Bottom-up Markov Chain Monte Carlo approach for scenario based residential load modelling with publicly available data. *Energy and Buildings* 2016; 112:121-129.
[13] Arun P, Banerjee R, Bandyopadhyay S. Optimum sizing of photovoltaic battery systems incorporating uncertainty through design space approach. *Solar Energy* 2009; 83(7):1013-1025.
[14] Roy A, Kedare SB, Bandyopadhyay S. Optimum sizing of wind-battery systems incorporating resource uncertainty. *Applied Energy* 2010; 87(8):2712-2727.
[15] Sharafi M, ElMekkawy TY. Stochastic optimization of hybrid renewable energy systems using sampling average method. *Renewable and Sustainable Energy Reviews* 2015; 52:1668-1679.
[16] Hagen B, Simonsen I, Hofmann M, Muskulus M. A multivariate Markov Weather Model for O&M Simulation of Offshore Wind Parks. *Energy Procedia* 2013; 35:137-147.
[17] Ramírez-Cobo P, Marzo X, Olivares-Nadal AV, Francoso JÁ, Carrizosa E, Fernanda Pita M. The Markovian arrival process: A statistical model for daily precipitation amounts. *Journal of Hydrology* 2014; 510:459-471.
[18] Yang H, Li Y, Lu L, Qi R. First order multivariate Markov chain model for generating annual weather data for Hong Kong. *Energy and Buildings* 2011; 43(9):2371-2377.
[19] Shamshad A, Bawadi M, Wanhussin W, Majid T, Sanusi S. First and second order Markov chain models for synthetic generation of wind speed time series. *Energy* 2005; 30(5):693-708.
[20] Ching W, Ng MK, Fung ES. Higher-order multivariate Markov chains and their applications. *Linear Algebra and its Applications* 2008; 428(2-3):492-507.
[21] Duffie JA, Beckman WA. *Solar engineering of thermal processes*. 4th ed. Hoboken, NJ: Wiley; 2013.
[22] Safner B. *Primärenergiefaktoren*, Schrift des BDEW Bundesverband der Energie- und Wasserwirtschaft e.V.; Berlin; 2015. 40 p.